A Non-Invasive Method for Hydration Status Measurement With a Microwave Sensor Using Skin Phantoms

Joni Kilpijärvi, Jarrkko Tolvanen, Jari Juuti, Niina Halonen, and Jari Hannu

***Abstract*—Fluid balance is important for a healthy human being. In this paper, a method to measure hydration status was developed and tested towards non-invasive measurement from human skin. Measurement of hydration status was performed by a microwave sensor utilizing a complementary split ring resonator (CSRR). The sensor was modeled, manufactured and then characterized by measuring tailor made skin phantoms based on the realistic electrical properties of skin with different degrees of hydration status. Qualitative longer term (>24 h) evaluation of the sensor was also performed by measuring polyester tissue that was drying over the time. Hydration status, represented by dehydrated, normal and hydrated skin phantoms, based on polyurethane with carbon and ceramic additives, was measured successfully by monitoring the changes in resonance frequency around 5.52 GHz. All results were compared to the dielectric reference measurements done by a commercial laboratory instrument.**

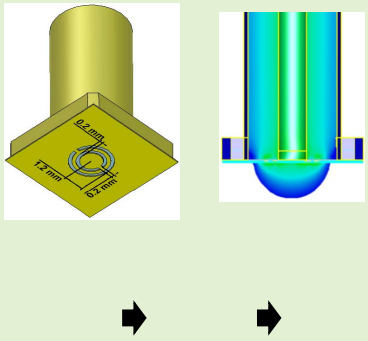

***Index Terms*—Microwave sensors, biomedical monitoring, dielectric measurement, skin phantoms, health monitoring.**

I. Introduction

THE human body contains large amounts of water depending on individual characteristics such as age and gender. Reduced water content may be the cause of many health problems, especially among children and elderly persons. Typical water content of the human body can vary from 55 wt.% up to 75 wt.%. [1] About 67 wt.% of the water can be located inside the cells (intracellular water) and 33 wt.% in tissue fluid (extracellular fluid). Moreover, water content is high in the blood (blood cells and plasma) and blood circulation is responsible for distributing and regulating the water to different locations in the body [2], [3].

At rest, more than half of the water loss takes place through urination, smaller portions through the skin (evaporation and sweating) and via the lungs (exhaling), saliva, and the remainder is lost through the intestinal canal (feces). Factors such as physical activity, consumed food, fluids and health problems can contribute to the water loss mechanisms. Lost water can be replenished by consuming fluid and food [2].

Regulation of the hydration status is vital for human health. When the system is not functioning correctly, mental and physical performance will be lower [4], [5]. The main regulation system for adjusting the hydration level in humans is the urinary system. Excess fluid in the body will be balanced by increased urination, whereas in dehydration the urine volume will be restricted. Urine volume can change from approximately 0.7 up to over 3 l/day [6]. In terms of bodily fluids one of the important factors is osmolality; this has a normal value around 275 to 290 mOsm/kg. If this level of osmolality is not met, a complex system involving sensor receptors, blood circulation system and kidneys starts to compensate, eventually leading to increased or decreased water loss through the urine. In cases of hydration deficiency, the sense of thirst would be activated leading to fluid intake among healthy individuals [2]. In addition to the body's own sensory system, it would be beneficial to monitor the water content of the body during the different activities in order to warn about the condition and mitigate problems of too low water levels.

The body fluids always contain ions which have importance in regulating the osmolality. The source of these ions (Na^+, Cl^- and K^+) is digested foods, and the ions have a large impact on the dielectric properties of water, especially

Manuscript received August 14, 2019; revised October 1, 2019; accepted October 2, 2019. Date of publication October 7, 2019; date of current version December 31, 2019. This work was supported by Proof of Concept (POC) funding, University of Oulu. The work of J. Kilpijärvi was supported by the Tauno Tönning Foundation. The associate editor coordinating the review of this article and approving it for publication was Prof. Guiyun Tian. *(Corresponding author: Joni Kilpijärvi.)*

The authors are with the Microelectronics Research Unit, Faculty of Information Technology and Electrical Engineering, University of Oulu, FI-90014 Oulu, Finland (e-mail: joni.kilpijarvi@oulu.fi; jarkko.tolvanen@oulu.fi; jajuu@ee.oulu.fi; niina.halonen@oulu.fi; jari.hannu@oulu.fi).

Digital Object Identifier 10.1109/JSEN.2019.2945817

at low frequencies, which is explained through the Maxwell-Wagner-Sillars effect. Relative permittivity can be found to be larger when the frequency is lower than 200 MHz. At higher frequencies the ion polarization diminishes because the ions are not able to respond to the applied external electric field. Since the relative permittivity of ions is typically lower than that of pure water, the permittivity of the mixture in this case is also lower than that of pure water. On the other hand, the ions increase the conductivity of the fluid, which causes greater dielectric losses than pure water up to 10 GHz [7]. To have an insight into the dielectric properties of a liquid with changing ion content, a blood phantom can be described. At 6 GHz saline water (NaCl) imitating the salinity of blood can change from 125 to 155 mmol, which corresponds to a change in relative permittivity from 70.2 to 69.7, in loss tangent from 0.355 to 0.370 and in conductivity (S/m) from 8.34 to 8.61, respectively. At 200 MHz, the corresponding values change from 80.6 to 80.55, 1.211 to 1.717 and 1.09 to 1.54 (S/m). It should be noted that the relative permittivity decreases ten times more at the higher frequency. The corresponding values for pure water change from 79.1 to 71.9, 0.0001 to 0.310 and 0.0001 to 7.45 S/m [8]. To evaluate body fluids as dielectric materials, for example, blood has a relative permittivity of 54 and a conductivity of 5.4 S/m at 5 GHz [9]. Blood permittivity is mostly related to water volume and its conductivity arises from the ions controlling the osmolality.

High frequencies can be highly beneficial for on-skin measurements due to the continuous perspiration through sweat glands that creates moisture on the skin. Respectively, DC and low frequency signals would be easily saturated due to conductive liquid (i.e. sweat) causing electric shorts on a sensor. However, at higher frequencies this is not as relevant since conductivity is increased by the ions having a lesser role at microwave frequencies and also microwaves can penetrate to the measured tissue (i.e. the skin).

Microwave sensors can be highly advantageous for water content measurements from tissue, due to the unique dielectric properties of water at high frequencies. Water molecules have a dipole moment due to their asymmetric shape. In addition, water molecules can easily move in the presence of an external electric field due to water's lower viscosity in the liquid phase in contrast to the solid phases. As a result, high relative permittivity can be seen even at high frequencies as water molecules can be orientated within the rapidly changing electric field. Also, dielectric losses will be high as the water molecules can absorb the electric field in the form of movement causing friction. Microwaves have been found to be strongly interactive with water, therefore enabling the development of various types of sensors [7].

Microwave sensors can be categorized in three main groups: reflection, transmission and resonator based structures. In a typical resonator sensor the electric field can be confined into a closed cavity. The electromagnetic waves having a standing wave pattern are dependent on the wavelength. In the presence of interference of the wave by a medium, a frequency shift of the standing wave can be observed, thus enabling measurement of the dielectric properties of the medium. If the medium has a high dielectric loss, the measurement accuracy can be limited but otherwise the method is typically considered as the most accurate way to measure dielectric properties [10]. In transmission sensors, the measurements are made through the medium, where the system typically consists of a transmitter and receiver. A large number of different kind of configurations have been presented, such as a moving transmitter/receiver or an array of receiver/transmitters systems, and even tomographic imaging has been used [11]. Reflection sensors have the simplest structures that have been found useful for many applications. Electromagnetic waves sent from the applicator can be measured as received reflected power. One simplified example would be a coaxial dielectric probe enabling measurements of dielectric properties of different materials. The sample in liquid or solid form is brought into contact with the open end of the coaxial transmission line. The sample changes the transmission characteristics due to the reflections and attenuation of the signal [12]. Coaxial line reflection sensors have been in use for several decades and commercial systems are available (e.g. Speag and Keysight). These systems are suitable systems for material dielectric characterization in a laboratory environment.

In this paper, a reflection sensor in combination with a resonator was used due to its versatile properties. The system requires one high frequency electrical connection for connecting the sensor to a measurement instrument that in many cases would be a vector network analyzer (VNA). The probe part of the sensor plays a critical role in making accurate measurements. The probe consists of a complementary split ring resonator (CSRR) pattern tuned to a specific high frequency [13]. The CSRR is well known from metamaterial applications due to its properties in interaction with an electromagnetic field. Capacitance and inductance values yielded by the CSRR can be very large even if the dimensions are small [14]. Therefore, a large diversity of sensing applications benefit from CSRRs, including gas, microfluidic and medical sensors [15]–[17].

In addition, other types of microwave sensors have been utilized for skin injury measurements [18], [19]. Hydration status measurements using microwaves have been done with antenna based sensors. A patch antenna (2-3 GHz) intended for wrist mounting with a passive reflector on the opposite side of the wrist was characterized using a liquid phantom by Tranz *et al.* [20]. Multi antenna (2-6 GHz) measurement located around the wrist in-vivo was presented in reference [21]. A more sophisticated, fully wearable system including the necessary electronics, operating at 2.45 GHz, was demonstrated in-vivo by Wang *et al.* [22]. A patent by Ionescu and Guerin [23] described a system consisting of a passive RF tag on the skin intended to be read by a mobile phone. Furthermore, a microwave sensor for a hydration measurement antenna, operating at 7-9.5 GHz, was used to measure cell culture in a bioreactor by Brendtke *et al.* [24]. A cellulose fiber substrate with integrated antenna (2-4 GHz) was also used to absorb and measure sweat for hydration monitoring in reference [25]. All these studies showed that microwave-based sensors have great potential for hydration status measurement. However, the authors note that no commercial, non-invasive, wearable devices exist for measuring

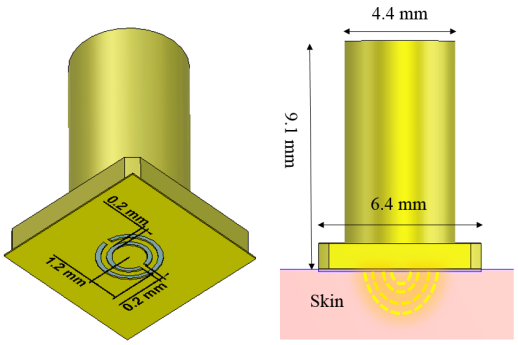

Fig. 1. Sensor design.

the hydration status of humans in real time, highlighting the importance of focusing on this both for research and eventually for modern health monitoring.

Herein, a sensor was developed for measuring the hydration status of a human body in real time directly from the skin utilizing a resonator designed to be placed in the vicinity of the skin. The design of the probe is presented in Fig. 1. To characterize the sensor in a laboratory environment, artificial skins with tuned dielectric properties (representing dry, normal, and moisturized skin), were manufactured by using four-phase polymer composites. The method of solid skin phantom manufacturing was adopted and modified from references [26], [27], whereas liquid phantoms have also been reported [20]. However, a solid medium enables a more realistic skin phantom model to be developed. It was expected for skin that the dielectric properties would be mostly related to blood plasma water content, which can change by up to ±14 % [28], [29]. The hypothesis was that dehydration leads to a lower water content in the skin with an increased ion content. Hydrated skin contains more water but less ions.

In addition, longer term testing of the sensor was performed by measuring wet fiber tissue as it lost it's moisture while drying with a resulting wide permittivity range.

II. Materials and Methods

A. Sensor Design

The developed microwave sensor was based on a CSRR, where the changing electromagnetic field causes a high intensity focal point on a specific site. The phenomenon enables a smaller size of the sensor and the selection of a specific resonance frequency. In addition, a large shift in resonance frequency occurs if the electrical properties change over the site of a high intensity electromagnetic field.

The sensor was optimized for detecting changes in the skin, while without the dielectric load of the skin the sensor lacks a characteristic resonance in the measured frequency band (100 MHz to 20 GHz). The footprint area of the sensor was aimed to have a minimum size for future integration into wearable devices such as bracelets or smartwatches. Moreover, a robust structure protecting the copper from oxidation and mechanical wear was achieved by using a urethane passivation layer on top of the sensor.

B. Simulation

CST STUDIO SUITE was used to model the sensor on skin. The simulation was performed using a time domain solver with automatic meshing (approximately 8.5 million mesh cells). All boundary conditions in the model were set open. The size of the ring resonator structure was optimized considering manufacturing restrictions and the desired frequency of around 5.5 GHz. The penetration depth of an electromagnetic wave is primarily related to its operating frequency. Typically, a lower frequency causes greater penetration due to the lower dielectric loss. The resonance frequency is related to the size of the resonator and the gap, which was 0.2 mm in this work (Fig. 1.). The larger the gap, the greater the penetration depth [30]. This is due to the larger gap causing a greater arching in the fringing field. Moreover, the difference in the relative permittivity can change the reflection behavior from the interface between the sensor and skin.

Dielectric properties for the simulation were acquired by using a Speag dielectric assessment kit (DAK) connected to a VNA (Rhode & Schwarz ZVB 20) at frequencies from 200 MHz to 20 GHz. The dielectric properties of skin (relative permittivity of 34.88 and dielectric loss 0.34) were acquired from reference [31] (also in tabulated form in reference [9]) and altered ± 5 % to obtain the dehydrated and hydrated values. Dehydrated skin was expected to have 5 % lower relative permittivity and 5 % higher loss due to the lack of water and the increased ion concentration. Hydrated skin was modeled with 5 % greater relative permittivity and 5 % smaller loss due to the larger volume of water. The dielectric range was also extended to see how the model behaved over a wider frequency range. The urethane passivation layer was simulated with a constant fit using a relative permittivity of 2.4 and dielectric loss of 0.02. Metal parts of the SMA connector were perfect electronic conductors (PEC) and the tape was simulated as lossy copper.

C. Sensor Fabrication

The sensor was manufactured seamlessly on a SMA connector. First, the legs were removed with pliers and the remaining surface was sanded to form a flat layer on the base. The surface was thoroughly cleaned with ethanol and isopropanol. Copper tape was carefully attached onto the crafted part and soldered to the sides of the SMA connector where the copper tape folded over the edge. A laser was used to cut the complementary ring oscillator pattern on the copper tape (LPKF ProtoLaser U3) and the cut parts were removed manually. Precise alignment was achieved by using the SMA connector's body as reference. Finally, the sensor surface was covered with urethane spray (Kontakt chemie, Uretahane 71) to form a robust structure. In addition, this fixed the copper tape firmly to the SMA connector as the inner insulator was made of Teflon forming a unified solid structure. To accelerate the curing and cross linking of the urethane, the structure was kept in a box oven at 60 °C overnight. The manufacturing process of the CSRR sensor is shown in Fig. 2.

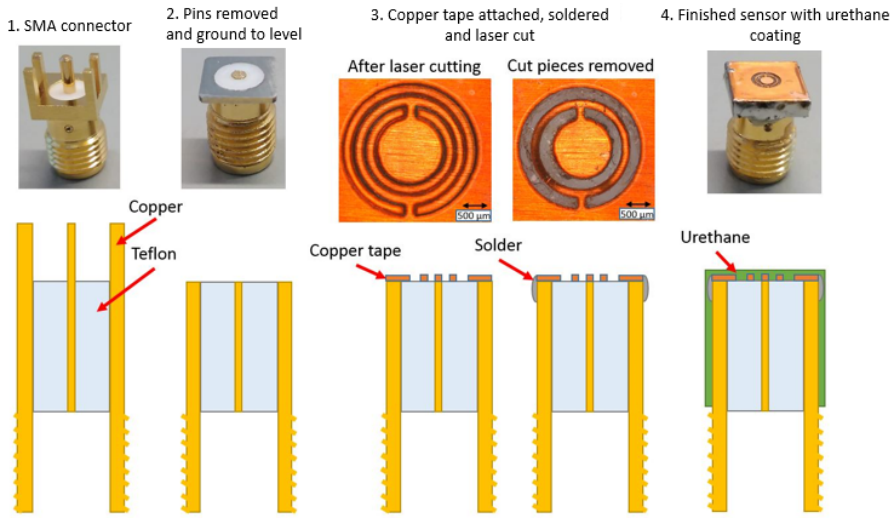

Fig. 2. Step-by-step manufacturing process.

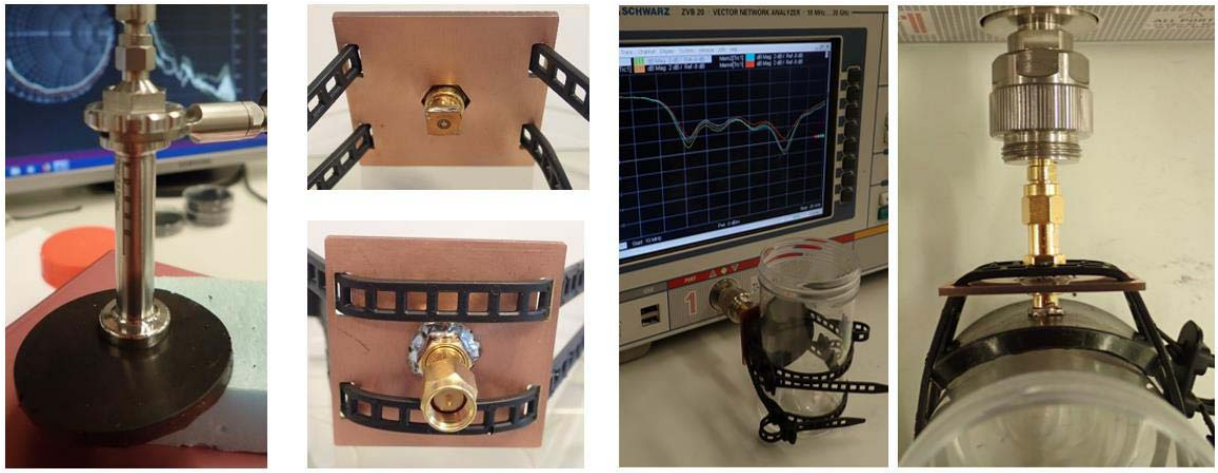

Fig. 3. (a) Dielectric property measurements of the skin phantom with DAK. (b) Sensor mounted on a wrist strap. (c) Measurement setup for the skin phantoms.

D. Measurement Setup and Calibration

Skin phantoms were measured using a Speag dielectric assestment kit (DAK) at a frequency range of 200 MHz to 20 GHz with 991 data points. Skin phantoms were placed on top of extruded polystyrene foam (Finnfoam) and raised up to achieve firm contact with the probe (Fig. 3a).

A PCB board resembling a wrist strap was manufactured with CNC (Roland RML). The sensor was mounted to a plug-plug SMA adapter soldered to a board (Fig. 3b). The skin phantoms were pressed against a plastic cylinder with diameter of 5.1 cm by using the wrist strap with two flexible zip ties (Fig. 3c).

The VNA (Rhode & Schwarz ZVB 20) was calibrated using an open-short-load protocol before all experiments. The proposed sensor was calibrated against the dielectric properties measured using the DAK in order to understand the resonance frequency shift *vs.* the dielectric properties change in different samples.

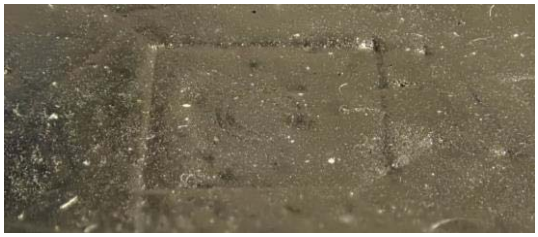

Fig. 4. Sensor features on the skin phantom after measurement.

E. Skin Phantoms

Vytaflex urethane rubber (Smooth-On Inc, Texas) was used as a polymer matrix. TIMREX SFG75 graphite powder (TIMCAL, Switzerland) together with VULCAN VX72 carbon black powder (Cabot, Massachusetts) and barium strontium titanate ($Ba_{0.65}Sr_{0.35}TiO_3$) were used as fillers for the four-phase polymer composites.

The skin phantoms based on urethane rubber-graphite/carbon black/barium strontium titanate composites

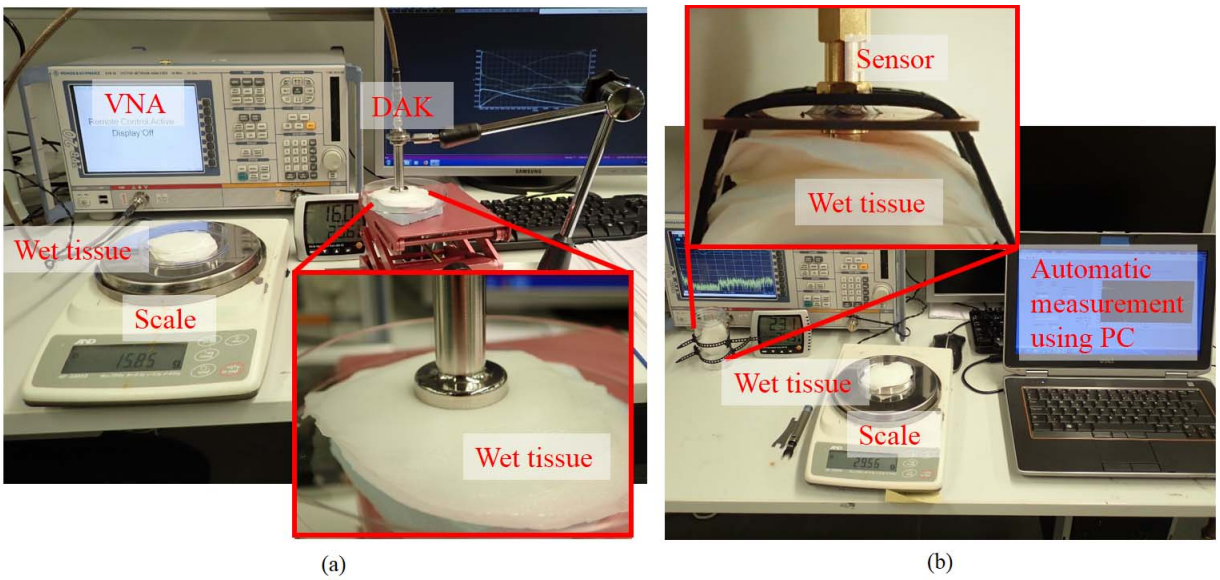

Fig. 5. Measurement setup for wet tissue experiment; with DAK (a) and proposed sensor (b).

were prepared with constant graphite and carbon black loadings of 24.3 and 8.2 wt.%, respectively, whereas the content of the BST was varied with 10, 12.5 or 15 wt.%. These phantoms are referred to as dehydrated skin (DS), normal skin (NS) and hydrated skin (HS), respectively. The composites were prepared at room temperature by hand stirring all the powders into urethane rubber A- and B-components (1A:1B) and applying numerous pouring and vacuum treatments for approximately 20 minutes to remove air bubbles, followed by curing at room temperature for 16-24 hours and post-curing for 4-8 hours in 65 °C before demolding.

The prepared skin phantoms were used for the characterization of the sensor as they mimic the dielectric properties of skin with different degrees of hydration status in the frequency range of 200 MHz to 20 GHz. Dehydrated skin has a lower permittivity and increased dielectric loss due to the loss of water and higher salt content in the leftover fluid, respectively. Conversely, hydrated skin has a larger permittivity and lower losses due to the increased water volume. Furthermore, it was shown that reliable electrical contact of the probe was achieved. The soft skin phantoms confirm features of the probe behaving similarly on a human skin (Fig. 4).

F. Wet Tissue Experiment

Longer term evaluation of the sensor was performed by measuring the moisture loss of a drying polyester tissue in an air-conditioned laboratory (23 °C, humidity 17%). Two identical samples were prepared from fiber tissue by cutting round pieces with diameter of 6 cm which were stacked to yield a total weight of 3.6 g. Then the tissues were soaked in distilled water yielding a total weight of 21.4 g per sample. The measurements were made in two stages, first with a DAK and afterwards with the developed sensor. The probes were pressed firmly to the surface of the samples to prevent physical movement during the drying process.

The weight of the sample was measured with a scale and in parallel the other identical sample was measured with the DAK. The setup can be seen in Fig. 5a-b. Similarly, the experiment was repeated with the sensor with the exception that the measurement data acquisitions were made by using a LabVIEW controlled VNA. This enabled continuous automatic measurement through the whole drying process.

III. Results

A. Simulation

In air no resonance peak could be found due to the small dimensions of the CSRR (in agreement with the simulations). However, when microwaves propagate into a medium having sufficiently high permittivity, the wavelength will be shorter fulfilling the resonance condition and producing characteristic resonance. With a bare SMA, as in Fig. 2 (process phase 2.), without the CSRR no resonance was observed in the used frequency band. The resonance phenomenon can be seen clearly in simulation of the different degrees of hydration status of the various skins. The value for normal skin was acquired from reference [31]. Dehydrated and hydrated values were estimated by changing the plasma volume. As the relative permittivity increased, the resonance frequency decreased, as seen in Fig. 6a (S11 simulation results).

The penetration depth of the electromagnetic waves was also studied by simulating the electric field maximum intensity in normal skin at the resonant frequency of 5.43 GHz. The waves achieved over 36 dB attenuation with a penetration depth of less than 1 mm (Fig. 6b). Penetration depth was similar for dehydrated and hydrated skin models.

B. Measurements

The dielectric properties of skin phantoms were characterized with the DAK and by using the developed sensor.

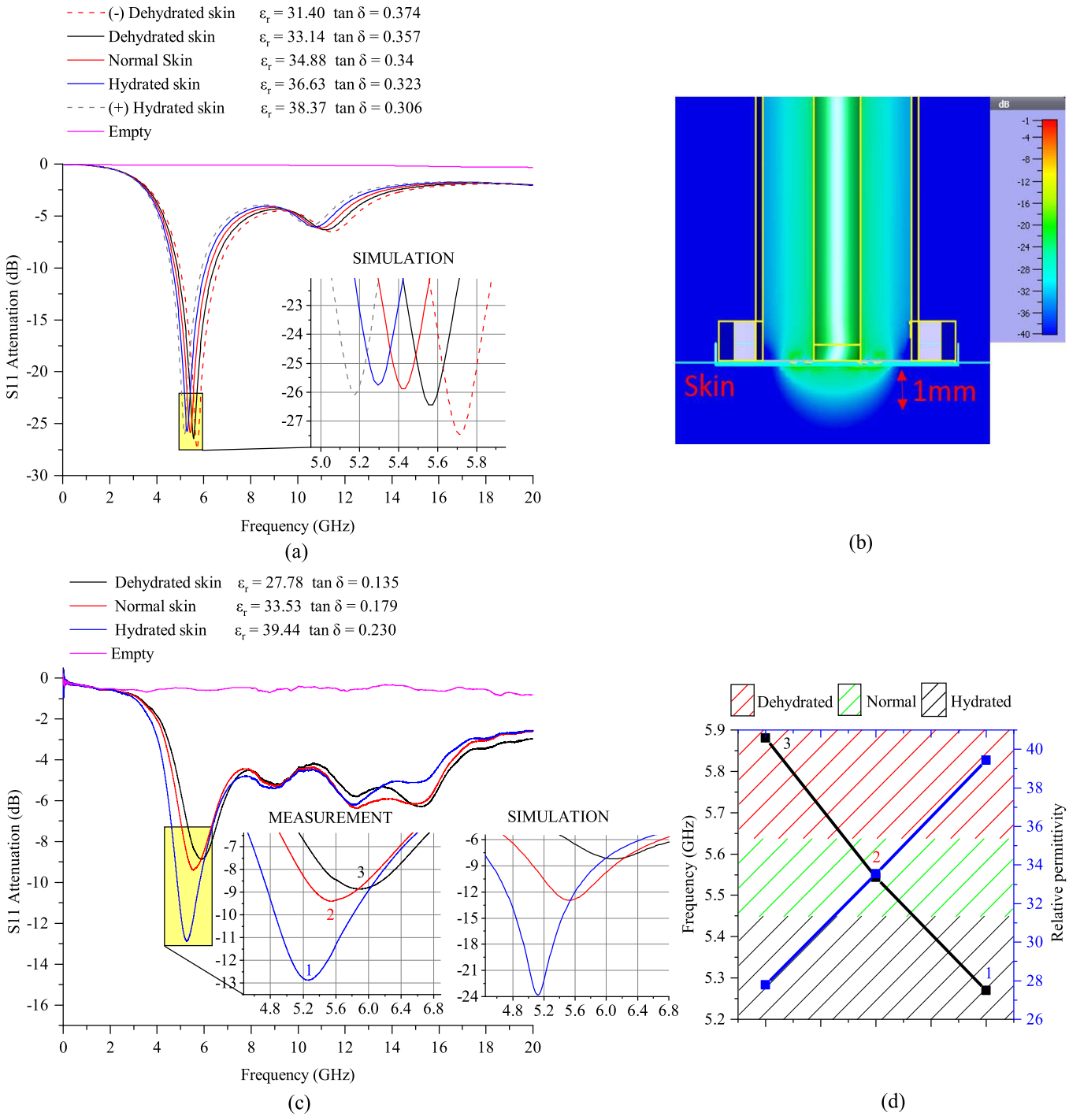

Fig. 6. Simulation results with different hydration status of skin (a), simulated signal attenuation in skin layer (b), measurement results with different skin phantoms, with corresponding simulation (c). Sensor response with skin phantoms vs DAK measured values (d).

Dielectric properties of the skin phantoms at 5.8 GHz and the measurement curves (S11) are shown in Fig. 6c. The measurements of skin phantoms (Fig. 6c) show similar behavior to that which was observed in the simulation results for human skin (Fig. 6a). To further analyze and verify the simulation, dielectric values of the manufactured phantoms were used to compare the modeled and the measured values (Fig. 6c). The simulation model correlated well with the results. Simulated and measured resonance frequency values were: hydrated skin 5.11 vs. 5.3, normal skin 5.53 vs. 5.52 and dehydrated skin 6.09 vs. 5.89 GHz.

Dielectric values for normal skin were acquired from reference [31]. Simultaneous adjustment of relative permittivity and dielectric loss within acceptable limits of skin were not possible for the developed composites. The relative permittivity is of utmost importance for the sensor response, thus it was the only parameter to be optimized. Moreover, according to the simulations, when the loss tangent changes from 0.135 to

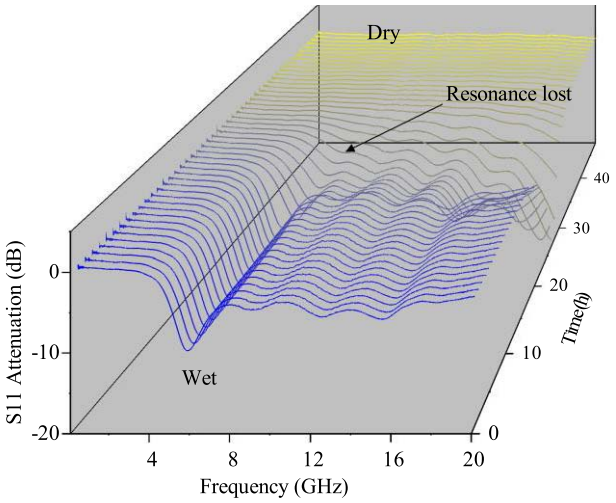

Fig. 7. Wet polyester wipes drying (1h steps between curves). Around 22 h the resonance was lost.

0.230, with constant relative permittivity of the NS phantom ($\varepsilon_r = 33.53$), it does not affect the resonance frequency, only the attenuation.

The resonance frequency was plotted against the DAK measured relative permittivity in Fig. 6d. The sensitivity of the sensor was calculated to yield 52 MHz $*\Delta\varepsilon_r$ with an excellent linear fit of $r^2 = 0.99$ (Coefficient of determination). This linear curve can be used for calibration of the sensor. The frequency resolution of the used VNA was 1 MHz.

Qualitative longer term (48 h) evaluation of the sensor was performed using an experiment with the drying of a wet tissue (Fig. 7). At the beginning, the tissue was found to be saturated with water causing a large relative permittivity. After 17 h the water had evaporated significantly. The loss of water in the tissue fibers caused a reduction in relative permittivity. Moreover, as the amount of total water evaporated from the tissues throughout the experiment, the relative permittivity decreased towards the permittivity of air, until the tissues had been completely dried of moisture to the level of the room humidity. It should be noted that the resonance was lost when the relative permittivity of the tissue reached about 20 at a time point around 22 h (Fig. 8a)

When comparing the sensor measurements to the DAK results, there is a clear correlation with the curves (Fig. 8a). As the weight of the tissue (Fig. 8b) and DAK values were recorded manually, there are some gaps in time. The curve has been extrapolated by using a Boltzmann fit, which is well suited for the drying phenomenon. First, the saturation phase (completely wetted) can be seen, that is followed by the fast drying phase, and when the sample approaches room humidity the drying slows down significantly (Fig. 8c). It should also be noted, that the drying times due to the evaporation, between the sensor and DAK were dissimilar due to the different size of the probe and orientation (proposed sensor horizontal and DAK vertical) giving only qualitative results. Regardless, the sensor showed a clear response with the drying sample as long as the resonance was lost.

In the first part of the measurement (0-12 h) the sensor showed a slowly increasing resonance frequency, which then started to increase rapidly behaving linearly up to a limit of where the resonance was lost. This shows that the sensor performed linearly in the relative permittivity range of 20 to 45, which is well within the permittivity range of real skin.

IV. DISCUSSION

The results show that there is a clear correlation between the measured resonance frequency and the measured dielectric properties. Results are easy to interpret and the hydration status can be determined. It was shown that the sensor was highly sensitive when the relative permittivity and loss tangent values were in the range of real skin. These limits were verified from the data acquired from the polyester tissue drying experiment. Moreover, there is a clear correlation between the simulated and measured values, thus the sensor performed as designed.

Earlier work on hydration measurement with microwaves has been performed with antennas. Successful and even portable systems have been presented. Comparison of different techniques can be seen on Table I. However, antennas have some drawbacks in their sensitivity, as there is a bulk effect from all the elements of the measured substances. For example, in the wrist there is skin, fat, muscle, bone and other types of tissue. The electromagnetic wave travels through all these materials producing a signal that is the sum of their dielectric properties, which can cause errors or hide relevant information derived from the skin. Moreover, the antennas can also pick up noise from the environment. In the future different techniques should be evaluated side by side in vivo to find out what is the best technique.

This work presents the first hydration status sensor utilizing microwaves with a split ring structure allowing the monitoring of changes of the resonance frequency and resulting in a very small physical size of the probe. The measured area is contained in skin Also, this study is the first time that solid phantoms have been used for mimicking hydration status. Overall, there is a clear indication that microwave sensors are suitable for measuring hydration status. The advantages are obvious compared to the Gold Standard of assessing hydration status, involving for example body mass change, urine tests, saliva, rating of thirst or isotope dilution techniques [32]. This is especially true when considering the ability to monitor the hydration status in real time through implementing microwave sensors.

Currently, the vector network analyzer is the most inhibiting factors for using this technology for real time continuous wearable and portable hydration status measurements. However, telecommunication technologies are progressing very rapidly, and new high frequency components are being developed for the Internet of Things, 5 G and eventually 6 G. It should be noted that many antennas (e.g. Bluetooth and GPS), including their electronics, have been integrated into wristwatches already. In the next generation of microwave hydration sensors, the VNA could be replaced with an integrated voltage-controlled oscillator (VCO) sweeping over the

TABLE I
COMPARISON OF DIFFERENT MICROWAVE MEASUREMENT TECHNIQUES

Technique	Dimensions	Operation	Frequency (GHz)	Sample	Output	Ref
Antenna and passive reflector	50 x 57 mm (antenna)	Reflection through wrist	2 - 3	Liquid (Blood phantom)	Phase/ Magnitude	[20]
8 antennas around wrist	-	Multi path transmission through wrist	2 - 6	In vivo, Wrist (only error analysis)	Magnitude	[21]
Two antennas and integrated electronics	-	Transmitting and receiving, wrist strap	2.45	Human experiment (n = 12)	Magnitude	[22]
RF-tag and mobile phone	-	RFID on skin	-	-	-	[23]
Antenna with cell culture	-	Reflection, cell culture on top	7 - 9	Cell culture	Frequency/ Magnitude	[24]
Paper substrate antenna	60 x 50 mm (antenna)	Reflection, paper absorbs sweat from skin	2 - 4	Liquid (Sweat phantom)	Frequency/ Magnitude	[25]
CSRR resonator	6.4 x 6.4 mm (resonator)	Reflection, resonator on skin, wrist strap	4.6 - 6.8	Solid (Skin phantom)	Frequency	This work

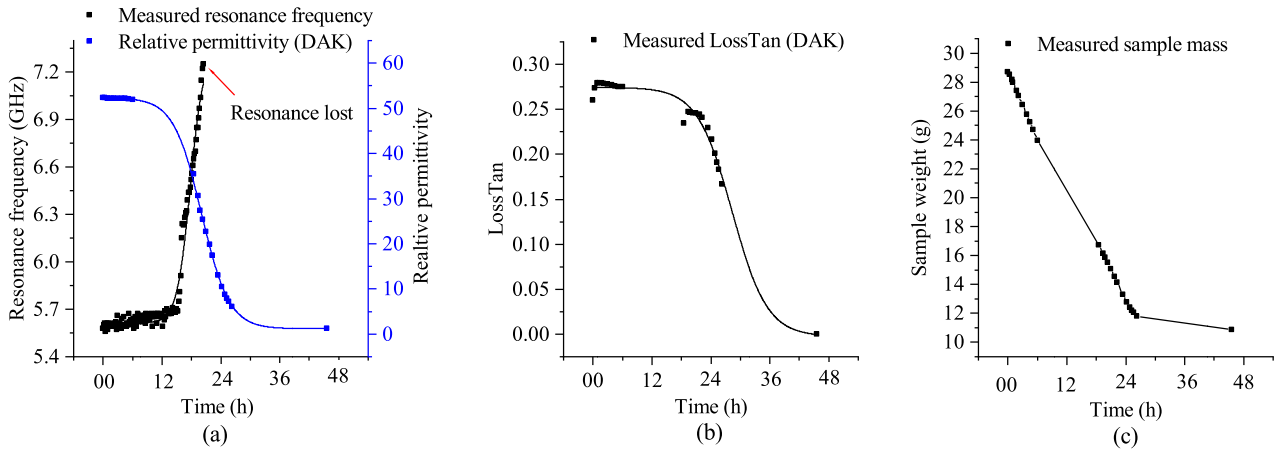

Fig. 8. Wet polyester tissue experiment with CSRR Sensor and DAK with measured data plotted as resonance frequency and relative permittivity (Boltzmann fit) (a), dielectric loss (Boltzmann fit) (b), and sample weight (c) vs time in hours.

designed resonance frequency. A VCO could be connected to the sensor and the power could be measured, for example, with off the shelf components (e.g. Analog devices, AD8318). The data could be sent to a mobile phone with Bluetooth for further processing.

The probe needs to be connected firmly to the skin without air gaps. If this criterion is not met, large measurement errors can be observed. This problem could be solved by introducing additional skin contact sensors, found in optical heart rate sensors (e.g. sports watches by Polar), where additional electrodes apply a small current, measure the resistance for optimal skin contact, and then record the heart rate. The force of the contact also plays a noticeable role. This could be solved by using a flexible bracelet keeping the force constant. It should also be noted that data relating to the dielectric values corresponding to the different degrees of hydration status of skin has not yet been collected from a sufficient number of test persons. The dielectric values used in this paper are based on the hypothesis of blood plasma increase or decrease.

Due to the individual characteristics of end users, the baseline for the normal hydration state needs to be initially established for the sensor. Then the baseline can be applied as a future reference. If the health status of the user changes, the baseline would need to be re-evaluated. This requires intelligent data analysis, where the users are considered as individuals with time-dependent variation. The baseline can be established in the long-run in a similar manner to that found nowadays in some sport watches, such as cardio load [33].

V. CONCLUSION

A sensor for measuring the hydration status of the human body was designed, modeled and manufactured. Moreover, solid skin phantoms mimicking the electrical properties of human skin were prepared for realistic characterization of the sensor. A qualitative longer term measurement was performed with the loss of moisture from a polyester fiber tissue. Results show that the proposed method could be suitable for wearable hydration status monitoring. However, clinical trials must be performed to verify the concept. Moreover, clinical trials could give more exact data on skin permittivity variation relative to hydration status.

ACKNOWLEDGMENT

The Center of Microscopy and Nanotechnology at the University of Oulu is acknowledged for technical support. Authors wish to thank Fab Lab Oulu for access to the CNC router.

REFERENCES

[1] E. Jéquier and F. Constant, "Water as an essential nutrient: The physiological basis of hydration," *Eur. J. Clin. Nutrition*, vol. 64, no. 2, pp. 115–123, 2010.
[2] B. M. Popkin, K. E. D'Anci, and I. H. Rosenberg, "Water, hydration, and health," *Nutrition Rev.*, vol. 68, no. 8, pp. 439–458, Aug. 2010.
[3] Z. Wang, P. Deurenberg, W. Wang, A. Pietrobelli, R. N. Baumgartner, and S. B. Heymsfield, "Hydration of fat-free body mass: Review and critique of a classic body-composition constant," *Amer. J. Clin. Nutrition*, vol. 69, no. 5, pp. 833–841, 1999.
[4] C. Cian, P. A. Barraud, B. Melin, and C. Raphel, "Effects of fluid ingestion on cognitive function after heat stress or exercise-induced dehydration," *Int. J. Psychophysiol.*, vol. 42, no. 3, pp. 243–251, 2001.
[5] B. Murray, "Hydration and physical performance," *J. Amer. College Nutrition*, vol. 26, pp. 542S–548S, Jul. 2007.
[6] W. F. Clark *et al.*, "Urine volume and change in estimated GFR in a community-based cohort study," *Clin. J. Amer. Soc. Nephrol.*, vol. 6, no. 11, pp. 2634–2641, 2011.
[7] E. Nyfors and P. Vainikainen, *Industrial Microwave Sensors*. Norwood, MA, USA: Artech House, 1989.
[8] J. Kilpijärvi, N. Halonen, J. Juuti, and J. Hannu, "Microfluidic microwave sensor for detecting saline in biological range," *Sensors*, vol. 19, no. 4, p. 819, 2019.
[9] P. Hasgall *et al.* (2018). IT'IS Database for Thermal and Electromagnetic Parameters of Biological Tissues, Version 4.0. IT'IS. [Online]. Available: https://www.itis.ethz.ch/virtual-population/tissue-properties/database/database-summary/
[10] M. S. Venkatesh and G. S. V. Raghavan, "An overview of dielectric properties measuring techniques," *Can. Biosyst. Eng.*, vol. 47, no. 7, pp. 15–30, 2005.
[11] C. Pichot, L. Jofre, G. Peronnet, and J.-C. Bolomey, "Active microwave imaging of inhomogeneous bodies," *IEEE Trans. Antennas Propag.*, vol. AP-33, no. 4, pp. 416–425, Apr. 1985.
[12] M. A. Stuchly and S. S. Stuchly, "Coaxial line reflection methods for measuring dielectric properties of biological substances at radio and microwave frequencies—A review," *IEEE Trans. Instrum. Meas.*, vol. IM-29, no. 3, pp. 176–183, Sep. 1980.
[13] J. B. Pendry, A. J. Holden, D. J. Robbins, and W. J. Stewart, "Magnetism from conductors and enhanced nonlinear phenomena," *IEEE Trans. Microw. Theory Techn.*, vol. 47, no. 11, pp. 2075–2084, Nov. 1999.
[14] D. R. Smith, S. Schultz, P. Markoš, and C. M. Soukoulis, "Determination of effective permittivity and permeability of metamaterials from reflection and transmission coefficients," *Phys. Rev. B, Condens. Matter*, vol. 65, no. 19, 2002, Art. no. 195104.
[15] A. Bogner, C. Steiner, S. Walter, J. Kita, G. Hagen, and R. Moos, "Planar microstrip ring resonators for microwave-based gas sensing: Design aspects and initial transducers for humidity and ammonia sensing," *Sensors*, vol. 17, no. 10, p. 2422, 2017.
[16] A. Salim and S. Lim, "Complementary split-ring resonator-loaded microfluidic ethanol chemical sensor," *Sensors*, vol. 16, no. 11, p. 1802, 2016.
[17] S. R. M. Shah *et al.*, "Penetration depth evaluation of split ring resonator sensor using *in-vivo* microwave reflectivity and ultrasound measurements," in *Proc. 12th Eur. Conf. Antennas Propag. (EuCAP)*, Apr. 2018, pp. 1–5.
[18] T. H. N. Dinh, S. Serfaty, and P.-Y. Joubert, "Bio-impedance non-contact radiofrequency sensor for the characterization of burn depth in organic tissues," *Proceedings*, vol. 2, no. 13, p. 780, 2018.
[19] F. Töpfer, L. Emtestam, and J. Oberhammer, "Long-term monitoring of skin recovery by micromachined microwave near-field probe," *IEEE Microw. Wireless Compon. Lett.*, vol. 27, no. 6, pp. 605–607, Jun. 2017.
[20] F. Trenz, V. Kalpen, R. Weigel, and D. Kissinger, "Modeling and measurement of a tissue-equivalent liquid for noninvasive dehydration sensing in the 2.45 GHz ISM-band," in *IEEE MTT-S Int. Microw. Symp. Dig.*, Sep. 2015, pp. 32–33.
[21] I. Butterworth, J. Serallés, C. S. Mendoza, L. Giancardo, and L. Daniel, "A wearable physiological hydration monitoring wristband through multi-path non-contact dielectric spectroscopy in the microwave range," in *IEEE MTT-S Int. Microw. Symp. Dig.*, Sep. 2015, pp. 60–61.
[22] J. Wang, Z. Zilic, and Y. Shu, "Evaluation of an RF wearable device for non-invasive real-time hydration monitoring," in *Proc. IEEE 14th Int. Conf. Wearable Implant. Body Sensor Netw. (BSN)*, May 2017, pp. 91–94.
[23] M. A. Ionescu and H. Guerin, "System for the remote monitoring of the hydration status of a living being," U.S. Patent 2016/0058364 A1, Mar. 3, 2016.
[24] R. Brendtke, M. Wiehl, F. Groeber, T. Schwarz, H. Walles, and J. Hansmann, "Feasibility study on a microwave-based sensor for measuring hydration level using human skin models," *PLoS ONE*, vol. 11, no. 4, Apr. 2016, Art. no. e0153145.
[25] A. R. Eldamak and E. C. Fear, "Conformal and disposable antenna-based sensor for non-invasive sweat monitoring," *Sensors*, vol. 18, no. 12, p. 4088, 2018.
[26] J. Garrett and E. Fear, "Stable and flexible materials to mimic the dielectric properties of human soft tissues," *IEEE Antennas Wireless Propag. Lett.*, vol. 13, pp. 599–602, 2014.
[27] B. Faenger, S. Ley, M. Helbig, J. Sachs, and I. Hilger, "Breast phantom with a conductive skin layer and conductive 3D-printed anatomical structures for microwave imaging," in *Proc. 11th Eur. Conf. Antennas Propag. (EUCAP)*, Mar. 2017, pp. 1065–1068.
[28] D. L. Costill, R. Coté, and W. Fink, "Muscle water and electrolytes following varied levels of dehydration in man," *J. Appl. Physiol.*, vol. 40, no. 1, pp. 6–11, 1976.
[29] F. Trenz, R. Weigel, and D. Kissinger, "Evaluation of a reflection based dehydration sensing method for wristwatch integration," in *Proc. 21st Int. Conf. Microw., Radar Wireless Commun. (MIKON)*, May 2016, pp. 1–3.
[30] P. M. Meaney, A. P. Gregory, J. Seppälä, and T. Lahtinen, "Open-ended coaxial dielectric probe effective penetration depth determination," *IEEE Trans. Microw. Theory Techn.*, vol. 64, no. 3, pp. 915–923, Mar. 2016.
[31] C. Gabriel, S. Gabriel, and E. Corthout, "The dielectric properties of biological tissues: I. Literature survey," *Phys. Med. Biol.*, vol. 41, no. 11, p. 2231, 1996.
[32] L. E. Armstrong, "Assessing hydration status: The elusive gold standard," *J. Amer. College Nutrition*, vol. 26, pp. 575S–584S, Jul. 2007.
[33] *Training Load Pro*. Accessed: Jul. 17, 2019. [Online]. Available: https://support.polar.com/en/training-load-pro

Joni Kilpijärvi received the B.Sc. and M.Sc. degrees in electronic engineering from the University of Oulu, Oulu, Finland, in 2015, where he is currently pursuing the Ph.D. degree with the Microelectronics Research Unit.

He is currently working on sensor research, especially focusing on human monitoring using microwave sensors. Presently, his interests are in developing novel sensors from start to finish, including modeling (electromagnetic simulation), manufacturing (polymer and ceramic materials, laser processing, and thin and thick film technology), measurements, and data processing.

Jarkko Tolvanen received the M.Sc. (Tech.) and D.Sc. (Tech.) degrees in electrical engineering from the University of Oulu, in 2015 and 2018, respectively.

Since graduation, he has been a Post-Doctoral Researcher with the Microelectronics Research Unit, University of Oulu. His current research interests include flexible and stretchable, biodegradable, and self-healing electronic materials and components, especially for wearable sensors.

Jari Juuti received the M.Sc. degree in mechanical engineering and the D.Sc. degree in electrical engineering from the University of Oulu, Finland, in 2000 and 2006, respectively.

He was appointed as a Docent/Adjunct Professor of Functional Materials their Components and Applications with the University of Oulu in 2009. From 2013 to 2018, he was an Academy Research Fellow of the Academy of Finland. He has contributed/supervised more than 35 research projects funded by the Academy of Finland, EU, ERC, Tekes, NICe, MATINE, and industry (additionally 20 privately funded commissioned research). He is the author of ∼100 refereed scientific journal publications, 17 conference articles, and three book chapters, and inventor of seven patents or patent applications. His research interests include piezoelectric materials, functional composites, actuators, motors and energy harvesters for micromechanical, and high frequency and printed electronics applications.

Dr. Juuti has been a Vice-Member of the Publications Committee of the University of Oulu, Series C Technica 2013–2018, and since 2019, a member and a series editor. He is a reviewer in ∼20 international journals.

Niina Halonen received the M.Sc. degree in organic chemistry and the Ph.D. degree in electrical engineering from the University of Oulu, Finland, in 2003 and 2013, respectively.

She is currently with the Microelectronics Research Unit, University of Oulu, as a Post-Doctoral Researcher and a Project Coordinator. Her research topics include nanomaterials, different sensor applications, and bio-based polymers.

Jari Hannu was born in Enontekiö, Finland, in 1980. He received the M.Sc. (Tech.) and D.Sc. (Tech.) degrees in electrical engineering from the University of Oulu, Finland, in 2006 and 2013, respectively.

From 2004 to 2006, he was a Research Assistant with the Department of Electrical and Information Engineering, University of Oulu, and continued as an Assistant and a Ph.D. Student. In 2007, he was a Visiting Researcher with the Centre of Micro and Nano Systems, Lancaster University, U.K. From 2012 to 2016, he was a University Teacher with the Microelectronics Research Unit, University of Oulu. From 2016 to 2017, he was the Chief Engineer of the Microelectronics Research Unit. Since 2017, he has been a University Lecturer with the Microelectronics Research Unit. Since 2016, he has also been the Director of the Degree Program of Electronics and Communications Engineering, University of Oulu. He is the author of more than 25 articles. His current research interests include electronics materials and its applications, especially in flexible devices and sensors, electronics testing technologies and reliability, and RF-sensing.

Dr. Hannu received Grants for his doctoral studies from the Finnish Foundation for Technology Promotion, the Nokia Foundation, the Seppo Säynäjäkangas Science Foundation, and the Riitta and Jorma Takanen Foundation, from 2006 to 2010. He received a Grant from the Ulla Tuominen Foundation in 2016 and a Proof-of-Concept Grant from the University of Oulu in 2018.